NACA RM E52H27

NACA

RESEARCH MEMORANDUM

INVESTIGATION OF RAM-JET AFTERBURNING AS A MEANS OF VARYING EFFECTIVE EXHAUST NOZZLE AREA

By Eugene Perchonok and Fred A. Wilcox

Lewis Flight Propulsion Laboratory
Cleveland, Ohio

NATIONAL ADVISORY COMMITTEE
FOR AERONAUTICS
WASHINGTON

November 17, 1952
Declassified December 3, 1958

1E

NATIONAL ADVISORY COMMITTEE FOR AERONAUTICS

RESEARCH MEMORANDUM

INVESTIGATION OF RAM-JET AFTERBURNING AS A MEANS OF VARYING EFFECTIVE EXHAUST NOZZLE AREA

By Eugene Perchonok and Fred A. Wilcox

SUMMARY

A discussion of the flow mechanism in an afterburner extension to a ram-jet engine is presented. Analysis indicated that with an afterburner, ram-jet performance equal to that of the engine equipped with a variable-geometry converging exit nozzle could result. The use of an afterburner requires, under some conditions, heat addition to a supersonic stream.

An experimental evaluation of the operation of a 16-inch ram jet equipped with an afterburner was conducted at Mach numbers of 1.8 and 2.0 in the Lewis 8- by 6-foot supersonic wind tunnel. The contraction ratio of the primary nozzle was 0.59 and of the secondary nozzle, 1.0. The experimental data confirmed the proposed method of afterburner operation. Although the combustion efficiencies of the primary and afterburner sections were lower than the general level of combustion efficiency of conventional ram jets, it was possible at a Mach number of 2.0 and with essentially no change in the diffuser-exit Mach number to increase the net internal thrust from 0.36 to 0.74 merely by increasing the total fuel flow.

INTRODUCTION

The flight paths of several proposed ram-jet-powered guided-missile configurations are such that engine operation during the boost phase is desirable. In addition it is usually advantageous to provide a thrust margin at the cruise Mach number for maneuvering purposes. With fixed-geometry nozzle configurations, such requirements cause off-design inlet diffuser operation which, in turn, is accompanied by total-pressure-recovery losses and drag increases.

A variable-geometry outlet is one method of dealing with this problem; however, the inherent mechanical complications make other means

of outlet flow control desirable. A second method is the use of a ram-jet afterburner which was proposed as a two-position variable exit in references 1 and 2.

The purpose of this report is to examine both analytically and experimentally the feasibility of using the afterburning ram jet to meet the requirements of variable-outlet-geometry operation. Included are experimental data for a 16-inch ram-jet engine equipped with an afterburner. These data were obtained in the Lewis 8- by 6-foot supersonic wind tunnel at Mach numbers of 1.8 and 2.0. Since the purpose of this investigation was to verify afterburner operation, no effort was expended in optimizing the configuration or raising the component combustion efficiencies.

SYMBOLS

The following symbols are used in this report:

A	area, sq ft
$C_{F,n}$	net internal-thrust coefficient
f/a	fuel-air ratio
K	constant
M	Mach number
P	total pressure, lb/sq ft absolute
p	static pressure, lb/sq ft absolute
R	universal gas constant
T	total temperature, $^{\circ}F$ absolute
sfc	specific fuel consumption, lb/hr/lb-thrust
$\Delta P/q$	flame-holder total-pressure-drop coefficient in terms of dynamic pressure at combustion-chamber inlet
γ	ratio of specific heat at constant pressure to specific heat at constant volume
η	combustion efficiency
μ	ratio of mass flow at combustor outlet to mass flow at combustor inlet

τ total-temperature ratio

Subscripts:

A ahead of normal shock

a afterburner

p primary combustor

t total or over-all

0 free stream

1 engine inlet

3 diffuser exit and combustion-chamber inlet

4 primary nozzle inlet

5 primary nozzle throat

6 primary nozzle outlet and afterburner inlet

7 engine exit

AFTERBURNER OPERATION

The afterburning ram jet is illustrated schematically in figure 1. It consists simply of a primary combustor, station 3 to station 4, and a converging-diverging nozzle, station 4 to station 6, followed by a constant-area afterburner, station 6 to station 7, and a second nozzle, station 7, which in figure 1 has a contraction ratio of 1. Both nozzle-throat areas depend on the engine-performance requirements; however, the throat area of the second nozzle must be larger than that of the primary nozzle.

As an aid in understanding afterburner operation, the typical variation of the thrust coefficient as well as the Mach numbers at stations tions 3 and 5 to 7 is given in figure 2 as a function of τ_a, the afterburner total temperature ratio. For efficient cruise operation, all heat addition is completed before the gases reach the throat of the primary nozzle, station 5. The velocity at the throat is sonic, and if a sufficient pressure ratio is available, the velocity of the gases in the afterburner section and at the engine outlet is supersonic.

In order to increase the thrust above the cruise value without changing the diffuser exit Mach number M_3, heat is added to the gases as they pass through the afterburner. The primary-combustor fuel-air ratio and consequently the primary-combustor total-temperature ratio τ_p, are maintained constant. A small amount of afterburner heat addition will decelerate the supersonic flow in the afterburner to a limiting Mach number of 1 at the throat of the second nozzle, station 7. When further heat is added, a normal shock forms in the region between station 5 and station 6 and the value of M_6, which depends on the primary-nozzle expansion ratio, drops from a supersonic to a subsonic value. Because of subsonic heat addition, the flow is then reaccelerated to M_7 of 1. With a constant-area afterburner, no change in thrust can occur until M_7 is 1 and the normal shock forms in the diverging section of the primary nozzle. As larger amounts of heat are added subsonically in the afterburner, the normal shock that forms initially at station 6 is driven toward the throat of the primary nozzle, station 5, and the thrust increases. With sufficient heat addition in the afterburner, M_5 becomes less than unity and further thrust increases are accompanied, as with the conventional engine, by a reduction in M_3 and off-design inlet operation. A one-dimensional analysis and a detailed discussion of the operation of a constant-area afterburner of the type described are given in the appendix.

APPARATUS AND PROCEDURE

The experimental verification of the operation of a ram-jet afterburner was made with a 16-inch ram-jet engine. The investigation was conducted at stream Mach numbers of 1.8 and 2.0 in the Lewis 8- by 6-foot supersonic wind tunnel with the same engine as used in reference 3. The coordinates of this engine are given in table I. As illustrated in figure 3, the engine was strut-mounted and a water-cooled pressure rake was used in determining the exit momentum.

In this preliminary investigation, advantage was taken of the high afterburner-inlet temperature and no afterburner flame holder was used. The primary combustor (fig. 4) consisted of a can-type flame holder identical with that used in reference 3 and was ignited by the flame of a vortex-type pilot burner, located in the downstream end of the centerbody. The pressure-drop variation across the can is given in figure 5.

Two primary-combustor fuel-injector configurations were required, one to obtain data below and the other above a M_3 of approximately 0.24 (fig. 4). Above a M_3 of approximately 0.24, a single-stage injector consisting of eight spray nozzles mounted in an annular manifold was used to introduce fuel into the can just downstream of the pilot. Below a M_3 of approximately 0.24, four nozzles were added to the original manifold and, in addition, a second annular manifold of 12 nozzles was used.

Afterburner fuel was injected through 12 nozzles mounted in an annular manifold and located between the end of the can combustor and the primary-nozzle entrance. Independent control was maintained over the afterburner fuel flow. Fuel-system details and spray nozzle types used are indicated in figure 4. Propylene oxide was used as fuel in both the primary combustor and the afterburner.

An existing graphite nozzle was used as the primary nozzle. A photograph of the installation is shown in figure 6 and nozzle coordinates and mounting details are given in figure 7. The contraction ratio investigated, 0.59, does not necessarily represent the optimum value.

Since the total length of the engine with afterburner was the same as the original engine without the afterburner (reference 3) the primary combustor was necessarily shortened in length by approximately 34 inches. Obviously, the combustion efficiency of the primary combustor will fall below the values reported in references 3 and 4, but since only the principle of the ram-jet afterburner was to be checked, no attempt was made to optimize the combustor.

The throat of the primary nozzle was initially located 5 inches downstream of the afterburner fuel injector, and the total afterburner length was $28\frac{3}{4}$ inches. Some data were also obtained with the afterburner fuel injector and the primary nozzle translated 10 inches downstream; thus an over-all afterburner length of $18\frac{3}{4}$ inches resulted.

The diffuser was operated supercritically at all times, and the engine air flow was computed from the diffuser inlet area and the tunnel stream conditions. The total fuel flow was determined with a rotameter, and orifice-type flowmeters were used to measure the fuel distribution to the primary combustor and afterburner fuel systems. A survey of the total and static pressures at the afterburner outlet was made with a water-cooled rake. Appropriate corrections for normal shock losses were made to the total-pressure measurements when the outlet flow was supersonic.

With the mass air flow, fuel flow, and exit total and static pressures known the exit Mach number, net thrust, over-all combustion efficiency, and over-all total-temperature-rise ratio were computed by methods conventionally used. The combustion efficiency is defined as the increase in enthalpy of the gases flowing through a combustor divided by the energy of the fuel available for combustion. Thus, in addition to afterburner fuel flow, the fuel unburned in the primary combustor is considered available for combustion in the afterburner.

The total-temperature ratio across the engine τ_t is based on pressure measurements made at the afterburner outlet. The total-temperature ratio across the primary combustor τ_p is computed from the relation (see reference 5)

$$M_3 \sqrt{\tau_p} = K \tag{1}$$

The value of the constant K was determined from the case of zero afterburner fuel flow and a temperature rise in the afterburner sufficient to just decelerate the flow to a M_7 of 1. (It was assumed that γ_6 was 1.35 and γ_7 was 1.28 in making this computation.) Thus, with K known, only M_3 was required to evaluate τ_p. When afterburner fuel was injected ahead of the primary nozzle, equation (1) was adjusted for the added mass. By the nature of the calculation, τ_p includes any effect due to vaporization or combustion of afterburner fuel occurring before the throat of the primary nozzle.

The total temperature ratio across the afterburner τ_a is computed from

$$\tau_a = \frac{\tau_t}{\tau_p} \tag{2}$$

Once the component temperature rise ratios τ_p and τ_a were known, the combustion efficiencies of both the primary combustor and the afterburner could be computed.

The experimental data presented herein are in terms of an internal-thrust coefficient. If it is desired to compute the propulsive thrust, the external drag coefficients at critical flow were 0.165 and 0.175 at stream Mach numbers of 2.0 and 1.8, respectively (reference 4).

RESULTS AND DISCUSSION

The performance trends observed experimentally generally agreed with the postulated afterburner flow mechanism; however, with the actual afterburner, some deviations from the theoretical trends were observed and will be discussed.

As predicted, large changes in thrust were observed at essentially constant diffuser-exit Mach numbers M_3 by merely increasing the afterburner fuel flow. The net internal-thrust variation for a typical transition region (operation between cruise and maximum thrust), M_3, 0.219±0.006 and M_0, 2.0, is given in figure 8 as a function of the total-temperature ratio across the engine. Also shown are the corresponding component total-temperature ratios across the primary burner and the afterburner, τ_p and τ_a. At the M_3 considered, the cruise fuel-air ratio was 0.057 (table II). During transition the primary f/a was reduced to 0.038 to give the same value of M_3.

The net thrust coefficient was increased from a cruise value of 0.36 to 0.74 with afterburning. Since τ_p remained essentially constant, the rise in τ_t was due to the heat added to the gases as they passed through the afterburner. Apparently some of the afterburner fuel burned in the primary combustor, because in order to obtain the same value of τ_p, a leaner primary fuel-air ratio f/a was required with the afterburner on than at cruise without afterburning (see table II), and in addition a very slight increase in τ_p was generally observed as the afterburner fuel flow was increased.

The M_3 at which transition occurred was a function of τ_p and, therefore, the primary f/a. The effect of the primary f/a on the transition M_3 at M_0 of 1.8 and 2.0 is shown in figure 9. Although the critical diffuser-exit Mach number at both stream conditions is approximately 0.20, it was felt that the minimum transition Mach numbers between 0.21 and 0.22 were sufficient to demonstrate afterburner operation.

According to the theory (see equation (1)), the transition M_3 at a given primary f/a should remain constant. Experimentally, however, a slight decrease in M_3 was observed as the thrust was raised by an increase in the afterburner fuel flow. This reduction in M_3 is due in part to the change in mass flow through the primary nozzle throat caused by the injection of afterburner fuel and in part to the burning of afterburner fuel in the primary combustor.

The maximum thrusts obtained with the afterburner at a M_0 of 2.0 have been compared in figure 9(b) with the theoretical and experimentally observed thrusts of the basic engine with the primary nozzle removed. The total engine length was held constant. The data indicate that the maximum thrusts observed with the afterburner-equipped engine fall below the equivalent fixed-geometry engine having an exit-nozzle-area ratio of 1. Although it is possible that the afterburner-equipped engine had not yet reached its maximum thrust limit (the maximum fuel flow was limited by the capacity of the pumping system), the flow losses caused by the primary nozzle will probably reduce the maximum thrust of this engine below that available from the equivalent fixed-geometry engine. It is also probable that the cruise thrusts obtained with the afterburner inoperative and fuel sprayed only through the primary injector will be slightly below the thrusts of the equivalent fixed-geometry cruise engine because of afterburner flow losses.

A detailed examination of the operation obtained in the primary as well as the afterburner combustion chambers is of interest. The data at a M_0 of 2.0 have therefore been reduced and are tabulated in table II. Although temperature-rise ratios across the engine τ_t as great as 3.9 were realized, the corresponding combustion efficiencies were quite low.

With supersonic flow in the afterburner, a maximum η_a of 22 percent was observed. With subsonic flow, the maximum η_a was 41 percent. Peak primary-combustor efficiency η_p was only 44 percent and maximum total combustion efficiency η_t was 52 percent. Although it may seem odd that the η_t is greater than either of the component efficiencies, this results from the definition of η_a which includes fuel unburned in the primary combustor.

For cruise operation, where an afterburner temperature-rise ratio of 1.0 is ideal, a τ_a of at least 1.25 was obtained. With the primary-nozzle expansion ratio that was used, this afterburner temperature ratio was sufficient to decelerate the supersonic inlet flow to an outlet Mach number M_7 of 1. During transition operation, temperature-rise ratios across the afterburner greater than those across the primary combustor were observed. Under high-thrust operation afterburner total-temperature ratios in excess of 2.0 resulted.

In order to indicate the specific fuel consumptions that may result with burner improvement, the actual specific fuel consumptions (based on net internal thrust) have been reduced to the value equivalent to 100 percent total combustion efficiency, and this ideal specific fuel consumption is listed in table II. At the same combustion efficiency, fuel comsumptions comparable with those of the basic engine with an exit-nozzle-area ratio of 1 were obtained with the afterburner-equipped engine. Moreover, instead of variation in the ideal specific fuel consumption with changes in thrust, as results for an engine with fixed outlet geometry, the ideal specific fuel consumption remained essentially constant during transition operation. At M_3 of 0.219 ± 0.006 for example, the thrust coefficient was more than doubled with very little change in the ideal specific fuel consumption. Thus, the afterburner may be used as the equivalent, with reasonable engine efficiency, of a continuously variable converging exit nozzle covering a range from cruise to the maximum thrust condition.

The variation of the total-pressure ratio across the engine as a function of M_3 is given in figure 10 for a M_0 of 2.0. Three theoretical curves are included in the figure. Two of these curves describe cruise operation (see appendix), one for the case without afterburning, $T_7/T_6 = 1$, and the other with sufficient afterburning to decelerate the flow to a M_7 of 1. The third theoretical curve applies to maximum thrust operation, $M_6 < 1$, $M_7 = 1$. The flame-holder pressure drop variation assumed in deriving these theoretical curves is indicated in figure 5.

Although no fuel was injected into the afterburner during cruise operation, energy liberated by fuel carried into the afterburner from the primary combustor made it impossible to obtain ideal cruise operation;

that is, $T_7/T_6 = 1$ (or $M_7 = M_6 > 1$). Agreement was observed, however, between the theoretical and experimental total-pressure ratios across the entire engine for the $M_7 = 1$ cruise data. The slight difference between the theoretical and the experimental curves probably represents the flow and burning losses through the primary nozzle, neither of which was included in the derivation of the theoretical curve. A similar difference between theory and experiment appears for the maximum-thrust data between a M_3 of 0.24 to 0.27. For a value of M_3 less than 0.24, it is not clear from the data whether or not, for the maximum thrusts recorded, the normal shock had been driven to the throat of the primary nozzle.

Because of the large pressure losses accompanying supersonic heat addition (see appendix) in the afterburner during cruise operation with $M_7 = 1$, the total-pressure ratio across the engine at cruise is less than the total-pressure ratio across the engine under maximum-thrust operation. Since cruise operation should be more efficient than high-thrust operation, this result appears, at first, incongruous. Because ideally the large afterburner total-pressure losses at cruise occur without a loss of momentum, they do not cause a reduction in either the cruise thrust or efficiency of the basic engine.

In order to avoid the unintentional heat addition in the afterburner during cruise operation, the primary nozzle was translated 10 inches downstream of its original position; thus an over-all afterburner length of $18\frac{3}{4}$ inches resulted. With this modification it was possible to reduce the heat addition in the afterburner and thus maintain supersonic velocities at the afterburner exit. The Mach number across the discharge jet varied from sonic at the center to values as high as 1.75 near the periphery, but the average values varied from 1.4 to 1.7.

The 0.59 primary nozzle contraction ratio results in over-expanded flow in the diverging section of the nozzle during ideal cruise operation. Because such over-expansion leads to a reduction in the cruise thrust, the selection of the primary-nozzle expansion ratio and the afterburner nozzle area may be dictated in part by flight conditions as well as thrust variation requirements.

Although these experimental results are preliminary, they are nevertheless sufficient to confirm the mode of operation proposed for a ram-jet afterburner and to demonstrate the practicability of obtaining large thrust changes with a fixed-geometry engine and at an essentially constant diffuser-exit Mach number merely by increasing the fuel flow. No air-flow or combustion-stability problems were encountered in changing from cruise to high-thrust operation. The thrust varied continuously in the transition region and could be maintained, if desired, at any intermediate value between cruise and maximum thrust.

Graphite proved a satisfactory primary nozzle material, and after several hours of operation there was no evidence of surface pitting or erosion of any kind. (The photograph of figure 6 was taken after approximately 4 hr of operation.)

Experience indicated that a single fuel system serving both the primary combustor and the afterburner may be adequate. However, more efficient combustion than obtained in this investigation is desirable.

In addition to the possibility of causing a reduction in the cruise thrust, it may be desirable to avoid the added weight and drag of the afterburner section during cruise operation. Since the maximum thrust for many applications will be required only during boost and acceleration to cruise periods, it may be possible to jettison the afterburner section during the cruise phase of the flight. An alternate method of operation may be to translate the primary nozzle into the afterburner section and thus take advantage of afterburner length for improved primary combustor performance during cruise operation.

Although the discussion has been concerned with the application of this system to a ram-jet engine, the same device may be applied to a turbojet engine requiring thrust variation and variable-exit-area control. This latter application may be as a second-stage afterburner or as a single-stage afterburner downstream of a choked nozzle.

CONCLUDING REMARKS

The preliminary investigation reported herein regarding the application of an afterburner to a ram-jet engine indicates that thrusts equal to those of the equivalent basic engine designed for either cruise or maximum thrust or any thrust value between these limits can be obtained merely by a variation in fuel flow. This large thrust variation (over 100 percent) was accomplished with only a negligible variation in diffuser-exit Mach number and therefore essentially no change in inlet flow or nacelle drag. The afterburner thus provides a fixed-geometry ram-jet engine with performance characteristics similar to those previously obtained only with a ram-jet engine equipped with a continuously variable exit nozzle.

The experimental observations confirm the theory proposed as an explanation for the operation of the afterburner. In addition, the data demonstrate that supersonic heat addition (burning) in a constant-area duct is not only physically possible but generally follows the relations derived from simple one-dimensional analysis.

Lewis Flight Propulsion Laboratory
National Advisory Committee for Aeronautics
Cleveland, Ohio

APPENDIX - ANALYSIS OF AFTERBURNER OPERATION

Because the addition of heat to a supersonic stream is encountered in the use of a ram-jet afterburner, constant-area supersonic heat addition must be considered in any analysis of afterburner operation. Although this mode of heat addition has been briefly treated in the literature (for example, reference 6), a more detailed analysis is desirable.

Assume a nonviscous, one-dimensional compressible fluid flowing in a constant-area duct from stations 1 to 2 such that M_1 and $M_2 > 1$ but that $T_2 > T_1$. From the conservation of momentum it can be shown that

$$\frac{p_2}{p_1} = \frac{1 + \gamma_1 M_1^2}{1 + \gamma_2 M_2^2} \tag{A1}$$

Combining equation (A1) with the expression for the conservation of mass between stations 1 and 2 gives in terms of the stagnation temperature

$$\mu^2 \frac{R_2}{R_1} \frac{T_2}{T_1} = \frac{\gamma_2 M_2^2}{\gamma_1 M_1^2} \left[\frac{1 + \gamma_1 M_1^2}{1 + \gamma_2 M_2^2}\right]^2 \left[\frac{1 + \frac{\gamma_2 - 1}{2} M_2^2}{1 + \frac{\gamma_1 - 1}{2} M_1^2}\right] \tag{A2}$$

Finally, when equation (A1) is expressed in terms of the total pressure, the following expression is obtained:

$$\frac{P_2}{P_1} = \left[\frac{1 + \gamma_1 M_1^2}{1 + \gamma_2 M_2^2}\right] \left[\frac{\left(1 + \frac{\gamma_2 - 1}{2} M_2^2\right)^{\frac{\gamma_2}{\gamma_2 - 1}}}{\left(1 + \frac{\gamma_1 - 1}{2} M_1^2\right)^{\frac{\gamma_1}{\gamma_1 - 1}}}\right] \tag{A3}$$

These expressions are generally given for the case of a subsonic initial Mach number ($M_1 < 1$), references 5 and 7, but they also apply for the supersonic case ($M_1 > 1$).

The solution of equations (A1), (A2), and (A3) for $M_1 > 1$ and both γ_1 and γ_2 equal to 1.3 is plotted in figures 11(a), 11(b), and 11(c), respectively. The simultaneous solution of equations (A2) and (A3) (fig. 11(d)) yields the variation in total-pressure ratio with initial Mach number and heat-addition parameter. The limiting condition (flow decelerated to sonic velocity) is shown as a dashed line. Supersonic flow is decelerated by constant-area heat addition and in the limit, the final Mach number M_2 reaches 1. The higher the initial Mach number, the larger the amount of heat the stream can absorb before deceleration to a M_2 of 1. In contrast to subsonic heat addition, a small amount of heat addition to a supersonic stream causes large total-pressure losses.

Another mechanism whereby a nonviscous, compressible fluid may be decelerated in a constant-area duct from a supersonic stream Mach number $M_1 > 1$ to $M_2 = 1$ is illustrated in the following sketch:

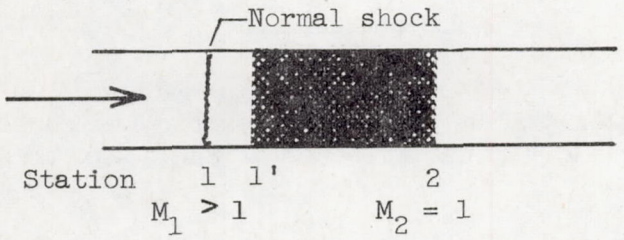

If a normal shock forms at station 1, the heat addition that begins at station 1' takes place at an initial Mach number $M_{1'} < 1$; sufficient heat is added to accelerate this subsonic stream to a M_2 of 1. Since the derivation of equations (A1) to (A3) did not require isentropic flow between stations 1 and 2, these same equations also describe this latter process.

It may therefore be concluded that in a constant-area duct, if the inlet flow is supersonic, the same heat-addition parameter is required for a final Mach number M_2 of 1, whether or not a normal shock is involved in the process. (A constant value of γ is assumed.) The values of the total- and static-pressure ratios and the heat-addition parameter between stations 1 and 2 may either be obtained from figure 11 or from the normal shock and subsonic heat-addition relations. In either case, identical values result.

Cruise operation. - In ideal cruise operation (fig. 12(a)), all primary-combustor heat addition is completed by station 5 and no heat is added in the afterburner. Thus, M_6 equals M_7 and if flow losses are

ignored, the afterburner exerts no influence on the thrust delivered by the basic engine. The primary nozzle contraction ratio determines the amount of heat addition required in the primary combustion chamber in order to obtain the design value of M_3. The primary nozzle expansion ratio selected must avoid overexpansion of the flow and the attendant thrust losses.

Transition operation. - Thrust increases with no change in the diffuser-exit Mach number may be obtained by adding heat to the gases as they flow through the afterburner section; however, before the maximum-thrust condition can be reached, the afterburner passes through a region of transition operation. This transition region occurs in two stages. Initially, heat is added to a supersonic stream.

$$M_5 = 1$$

$$M_6 > M_7 > 1$$

and because momentum is conserved, no thrust change is observed. This condition is shown schematically in figure 12(b).

In deriving the pressure, temperature, and Mach number relations that describe afterburner operation (fig. 13), nonviscous, one-dimensional, compressible flow was assumed. It was further assumed that all afterburner heat addition occurred between stations 6 and 7 and that

$$T_6/T_5 = 1$$

The ratio of the specific heats γ was held constant at 1.3.

The theoretical relation between the heat-addition parameter $\mu^2 \frac{R_7}{R_6} \frac{T_7}{T_6}$ and M_7 (where $M_7 > 1$) is given in figure 13(a) for several primary-nozzle-expansion ratios. At any given primary-nozzle-expansion ratio A_5/A_6 the addition of heat to the supersonic stream causes a flow deceleration, and in the limiting case, the stream can be decelerated to a final Mach number M_7 of 1 (fig. 12(c)).

During cruise operation of an actual engine, burning is usually not yet completed at the throat of the primary nozzle, and some heat addition may occur in the afterburner. If this is the case, the engine will actually be operating in the first stage of the transition region.

At the condition of sufficient afterburner heat addition to obtain a M_7 of 1, the process can be either heat addition to a supersonic stream or, as previously indicated, a normal shock at station 6 followed by subsonic heat addition. The values of the heat-addition parameter and the

total- and static-pressure ratios are identical for both cases. At a given primary-nozzle-expansion ratio, the addition of more heat than that indicated in figure 13(a) at a M_7 of 1 will cause a normal shock to form at station 6 and be driven toward station 5. This is the second stage of transition operation and is indicated schematically in figure 12(d).

The occurrence and exact position of the shock depend on the primary-nozzle-expansion ratio and the value of the heat-addition parameter. The relation between the Mach number at which the shock occurs M_A, the primary-nozzle-expansion ratio A_5/A_6, and the afterburner heat-addition parameter, is easily computed from the one-dimensional flow and heat-addition relations (fig. 13(b)). It is clear that more heat can be added in the afterburner as the ratio A_5/A_6 is reduced or as M_A, and consequently M_6, is lowered.

The total-pressure ratio across the afterburner in the second stage of transition operation may be computed by adding the loss across the normal shock occurring at M_A to the loss across the constant-area duct, stations 6 to 7, due to subsonic heat addition. The loss due to friction is neglected. The pressure ratio P_7/P_A or equivalently P_7/P_5 is plotted in figure 13(c). For convenience, these data are also presented as a function of M_A and A_5/A_6. At a given M_A the loss in total pressure due to a large variation in A_5/A_6 is small. However, large total-pressure losses are encountered as the normal shock occurs at successively higher values of M_A.

In applying this region of afterburner operation to an actual engine, it would be expected that the thrust delivered would increase continuously from the cruise value to the maximum-thrust condition at M_A of 1. Moreover, because the heat addition in the primary combustor is held constant the diffuser can be operated at its design point throughout this thrust variation. If the engine is operated at other than design flight Mach number, the primary combustor heat input should correspond to the M_3 value yielding optimum diffuser performance.

High-thrust condition. - At the diffuser-outlet Mach number M_3 selected as the design value, greatest thrust occurs when sufficient heat is added in the afterburner to drive M_A to 1 at station 5 (fig. 12(e)). When primary-nozzle flow losses are neglected, this thrust is equivalent to the thrust delivered by a fixed-geometry engine with an exit-area ratio of 1.

Even greater thrust is possible by increases in the heat released in the primary combustor or in the afterburner (heat addition greater than that for M_A of 1). However, in either case, the value of M_3 will be reduced and, if the engine is designed for critical diffuser operation, will be accompanied by an increase in external drag.

REFERENCES

1. Anon.: Booster Ram Jet Study. CAE Rep. No. 375, Continental Aviation and Engineering Corp. (Detroit, Michigan), Nov. 29, 1948. (Contract W-33-038-ac-13371.)

2. Minton, S. J.: Study of Self-Acceleration Potentialities of Ramjet Engines. Rep. No. 5145, Proj. 20-108, Marquardt Aircraft Co. May 22, 1951. (Contract W-33-038-ac-19050, E.O. No. 506-150.)

3. Perchonok, Eugene, Wilcox, Fred, and Pennington, Donald: Effect of Angle of Attack and Exit Nozzle Design on the Performance of a 16-Inch Ram Jet at Mach Numbers from 1.5 to 2.0. NACA RM E51G26, 1951.

4. Nussdorfer, T., Wilcox, F., and Perchonok, E.: Investigation at Zero Angle of Attack of a 16-Inch Ram-Jet Engine in 8- by 6-Foot Supersonic Wind Tunnel. NACA RM E50L04, 1951.

5. Perchonok, Eugene, Sterbentz, William H., and Moore, Stanley H.: Indirect Methods for Obtaining Ram-Jet Exhaust-Gas Temperature Applied to Fuel-Metering Control. NACA RM E7H27, 1948.

6. Hicks, Bruce L.: Addition of Heat to a Compressible Fluid in Motion. NACA ACR E5A29, 1945.

7. Hawthorne, W. R., and Cohen, H.: Pressure Losses and Velocity Changes Due to Heat Release and Mixing in Frictionless, Compressible Flow. Rep. No. E.3997, British R.A.E., Jan. 1944.

TABLE I - 16-INCH RAM-JET ENGINE COORDINATES

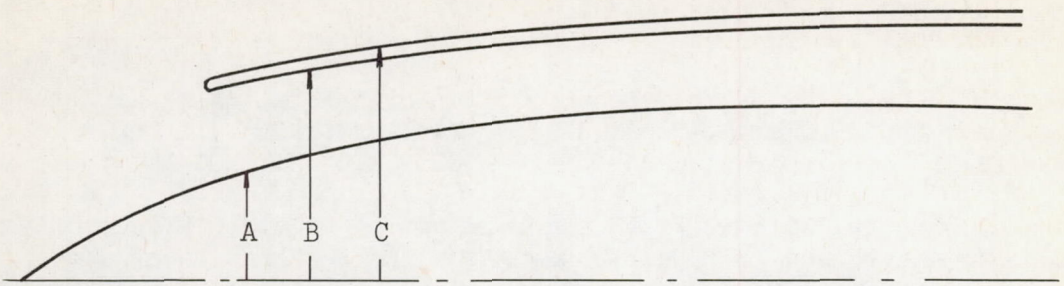

Station (in.)	Location	A (in.)	B (in.)	C (in.)	Miscellaneous
-5.05	Tip of spike	0			
-4.0		0.48			
-3.0		0.94			
-2.0		1.41			
-1.0		1.88			
0	Lip of inlet	2.34	5.05		Lip radius 0.032
1.0		2.78	5.13	5.37	
2.0		3.10	5.30	5.54	
3.0		3.36	5.45	5.69	
4.0		3.58	5.59	5.83	
6.0		3.94	5.83	6.07	
8.0		4.21	6.03	6.28	
10.0		4.40	6.20	6.45	
12.0		4.52	6.36	6.61	
14.0		4.58	6.48	6.72	
16.0		4.60	6.58	6.82	
18.0		4.58	6.61	6.85	
30.0		4.44	Straight	Straight	
46.0		4.02	taper	taper	
59.0		3.08	7.75	8.13	
63.0		2.43	7.45		
68.4	End of center body	0	7.38		
81	Pilot air inlets	1.5			
93	Pilot maximum diameter	4.0		Cylindrical section	
107	Station 3	3.3	8.00		
148	Primary nozzle inlet				
187	Engine exit		8.00	8.13	

NACA

TABLE II - INTERNAL ENGINE PERFORMANCE AT FREE-STREAM MACH NUMBER OF 2.0.

[Diffuser-exit static temperature, 162° ±2° F; diffuser-exit static pressure, 2475 ±325 lb/sq ft]

Fuel-air ratio f/a		Percent fuel to primary	Diffuser exit Mach number M_3	Net internal thrust coefficient $C_{F,n}$	Combustion efficiency			Temperature ratio			Specific fuel consumption	
Primary	Over-all				Primary η_p	After-burner η_a	Total η_t	Primary τ_p	After-burner τ_a	Total τ_t	Actual sfc	Ideal $(sfc)\eta_t$
0.076	0.076	100	0.212	0.46	0.27	0.16	0.39	2.41	1.25	3.02	8.44	3.30
.066	.066	100	.218	.40	.28	.17	.41	2.30	1.25	2.88	8.33	3.39
.057	.057	100	.225	.36	.28	.19	.42	2.18	1.25	2.73	8.08	3.41
.050	.050	100	.232	.30	.28	.20	.43	2.05	1.25	2.56	8.61	3.67
.043	.043	100	.238	.25	.29	.21	.44	1.95	1.25	2.43	8.72	3.85
.032	.032	100	.258	.14	.27	.22	.44	1.68	1.25	2.10	12.18	5.32
.012	.087	14	.262	.50	.40	.32	.37	1.41	2.21	3.12	8.83	3.26
.012	.079	16	.267	.48	.36	.33	.39	1.37	2.23	3.06	8.46	3.27
.012	.070	18	.273	.39	.33	.32	.37	1.34	2.08	2.78	9.30	3.41
.012	.066	19	.280	.30	.27	.28	.32	1.28	1.96	2.51	11.01	3.57
.019	.101	19	.248	.56	.36	.29	.35	1.55	2.11	3.27	9.14	3.22
.019	.087	22	.255	.53	.34	.32	.39	1.51	2.14	3.23	8.37	3.26
.019	.076	25	.263	.43	.29	.30	.37	1.44	2.02	2.91	9.04	3.33
.019	.066	28	.270	.25	.25	.22	.28	1.39	1.68	2.34	13.40	3.79
.025	.063	40	.237	.51	.42	.40	.52	1.86	1.77	3.30	6.35	3.32
.025	.082	31	.233	.64	.42	.40	.50	1.85	2.00	3.70	6.48	3.25
.025	.092	28	.228	.67	.44	.36	.47	1.90	1.98	3.76	6.97	3.27
.025	.075	34	.233	.61	.43	.41	.52	1.89	1.66	3.11	6.19	3.25
.038	.108	36	.213	.74	.39	.32	.44	2.16	1.83	3.95	7.39	3.28
.038	.099	38	.216	.71	.39	.33	.46	2.13	1.82	3.87	7.14	3.30
.038	.087	44	.218	.68	.39	.36	.50	2.14	1.78	3.81	6.56	3.28
.038	.066	58	.222	.51	.39	.33	.50	2.14	1.53	3.27	6.59	3.31

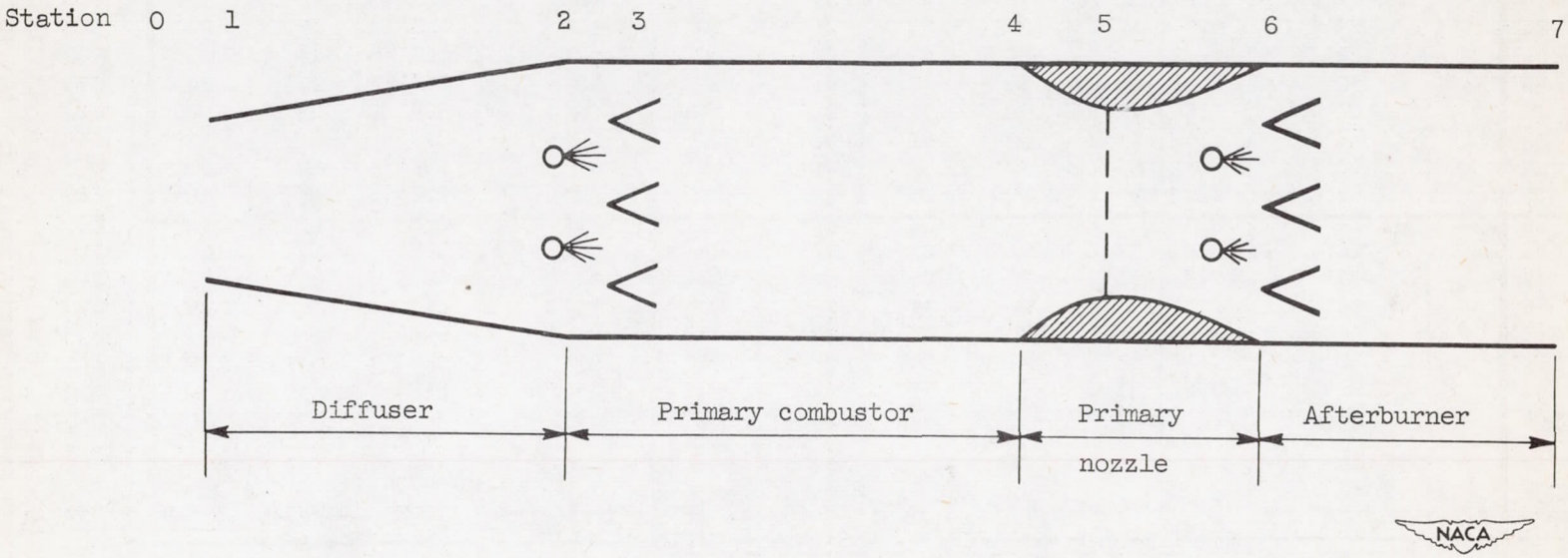

Figure 1. - Schematic diagram of afterburner-equipped ram-jet engine.

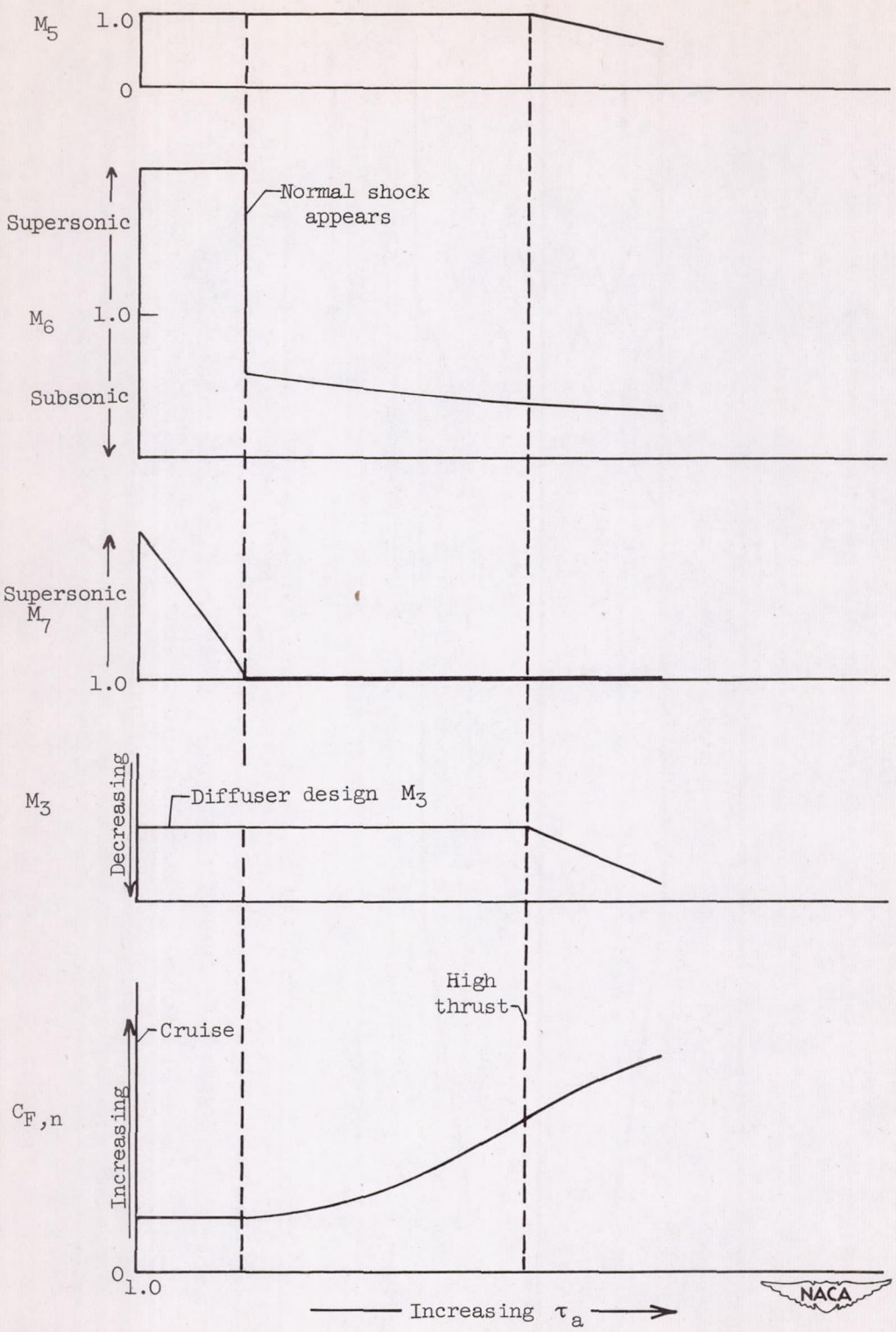

Figure 2. - Predicted effect of afterburner heat addition on thrust coefficient $C_{F,n}$ and internal Mach numbers M_3, M_5, M_6, and M_7.

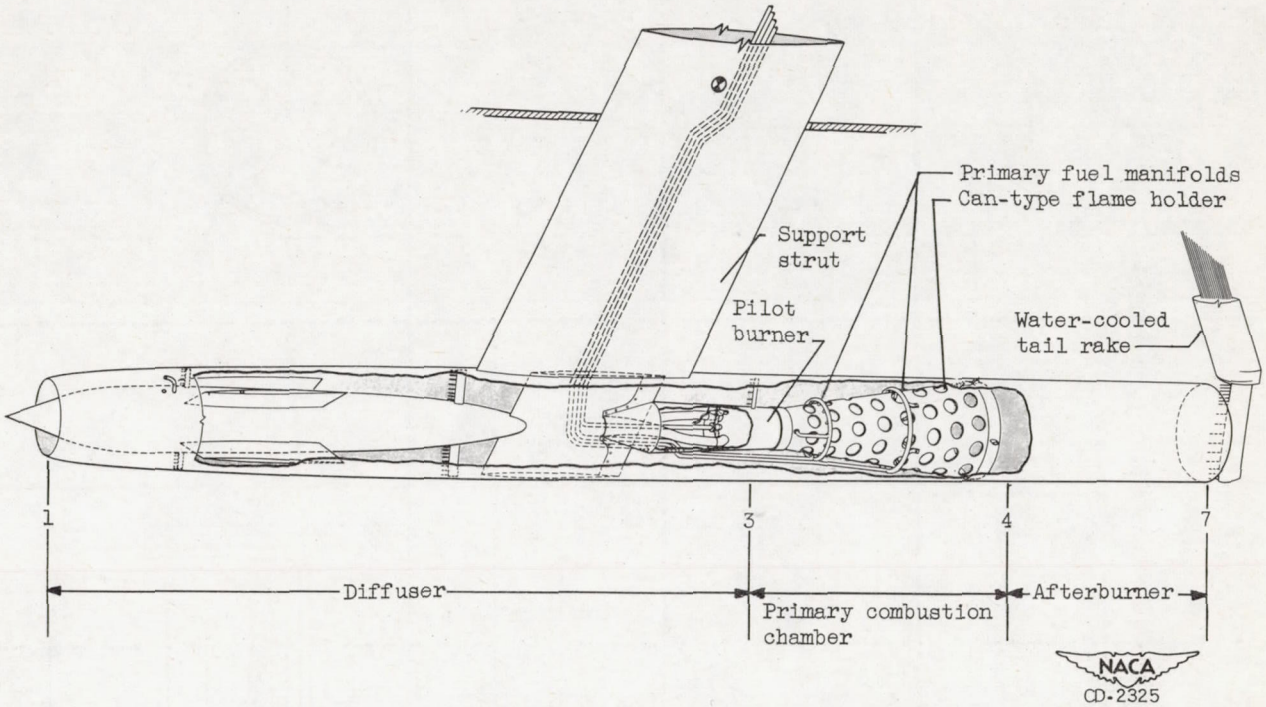

Figure 3. - Schematic diagram of 16-inch ram jet engine.

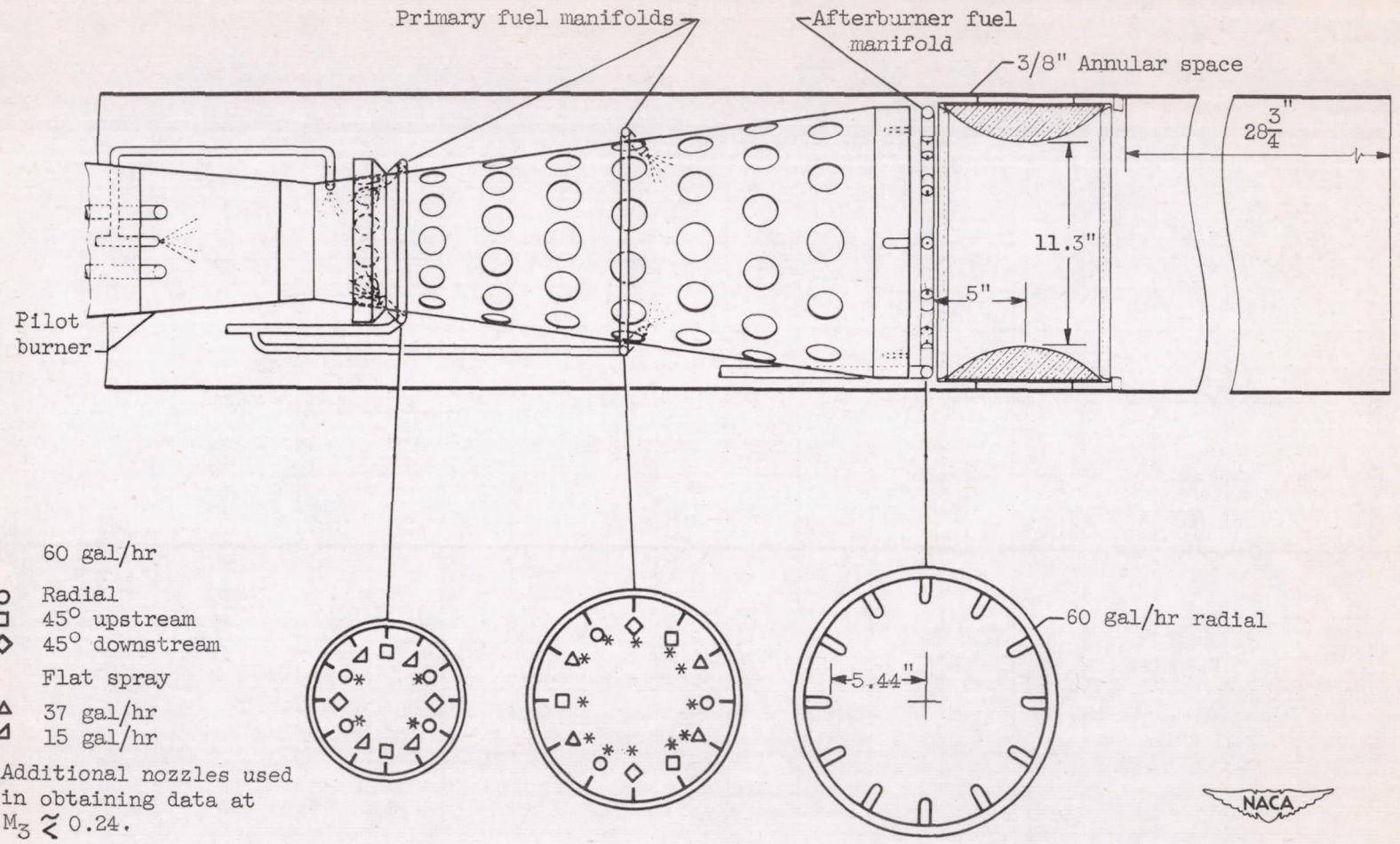

Figure 4. - Schematic diagram of combustor and afterburner details.

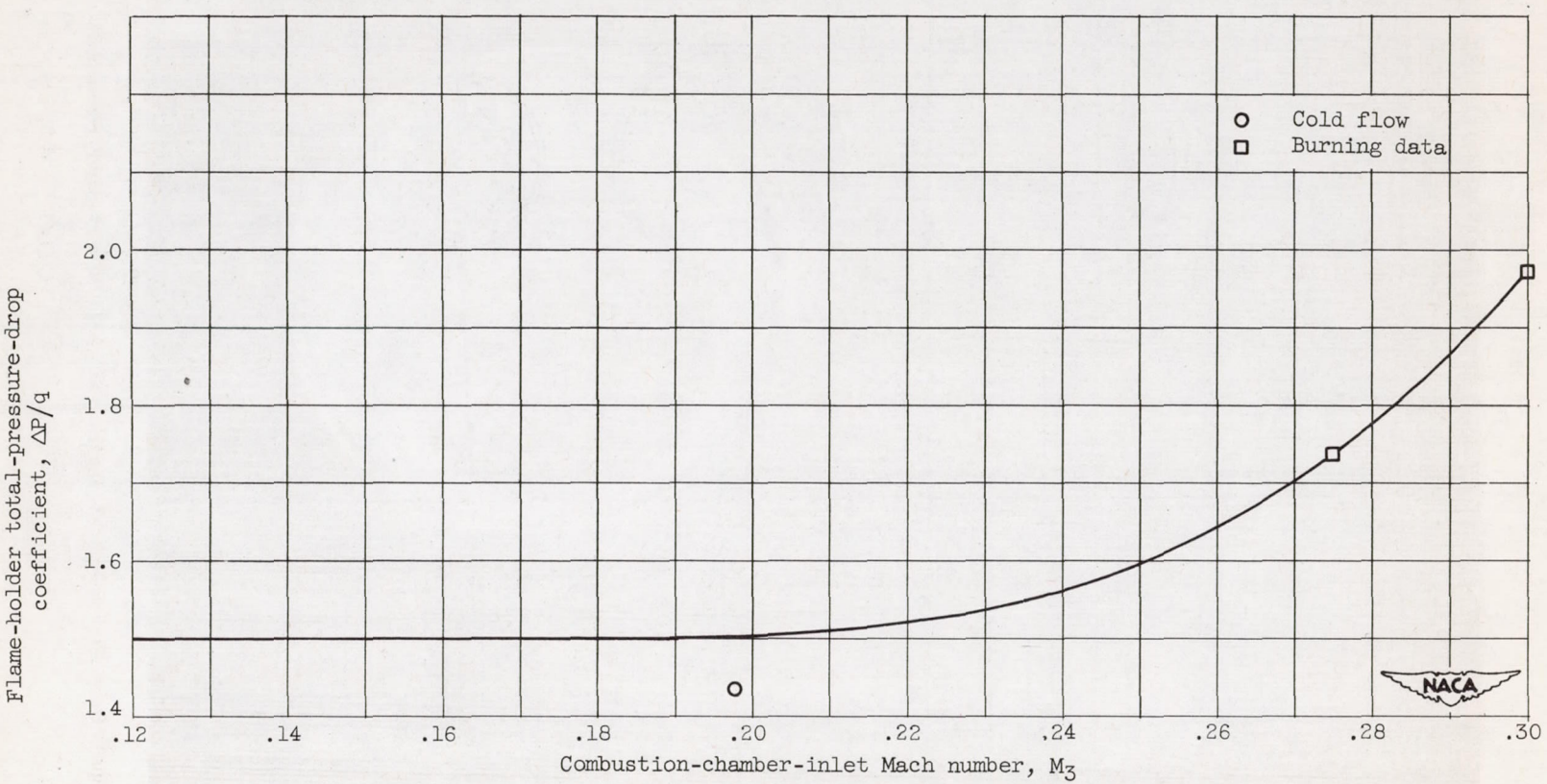

Figure 5. - Flame-holder pressure-drop variation.

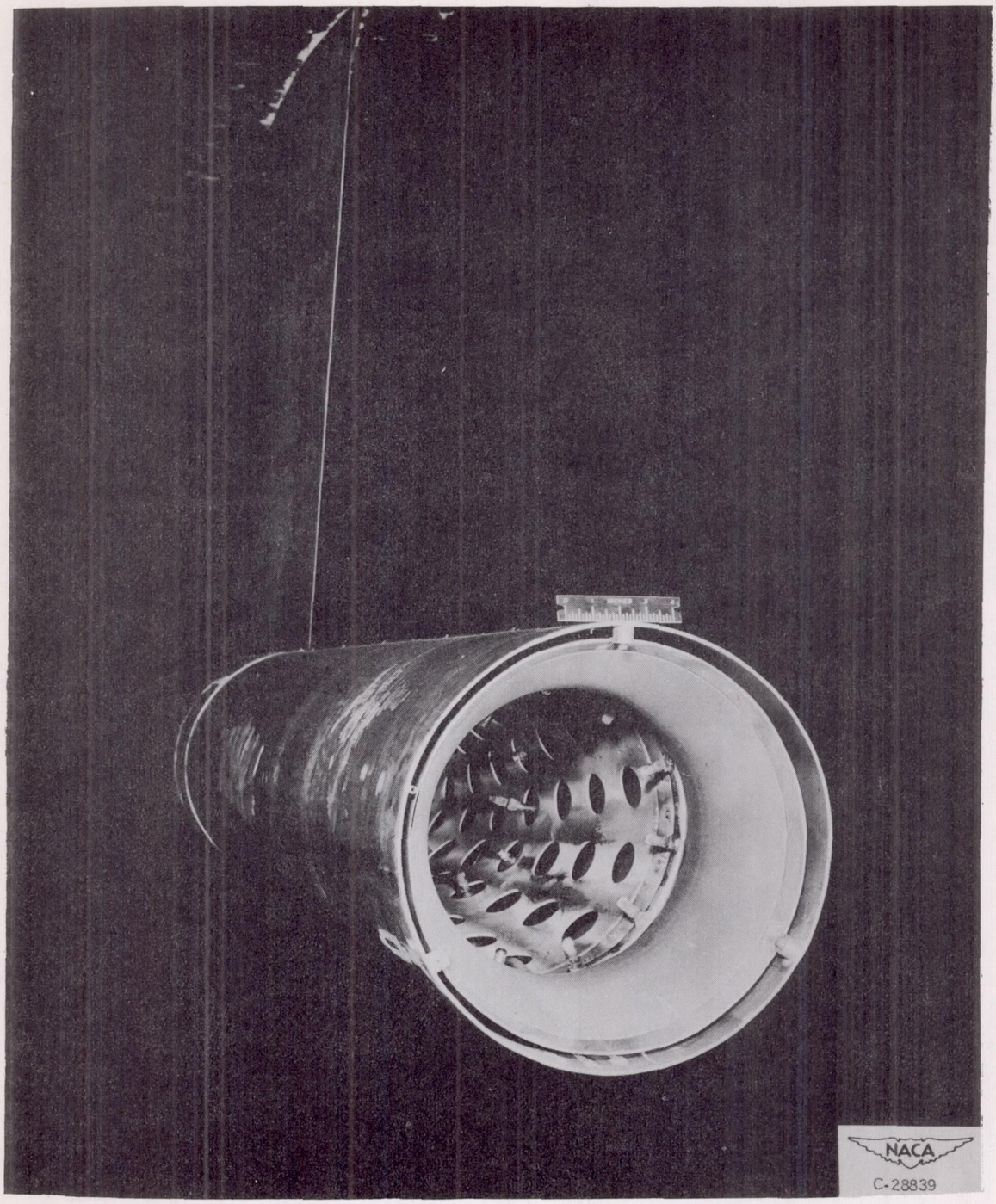

Figure 6. - Photograph of engine exit with afterburner removed.

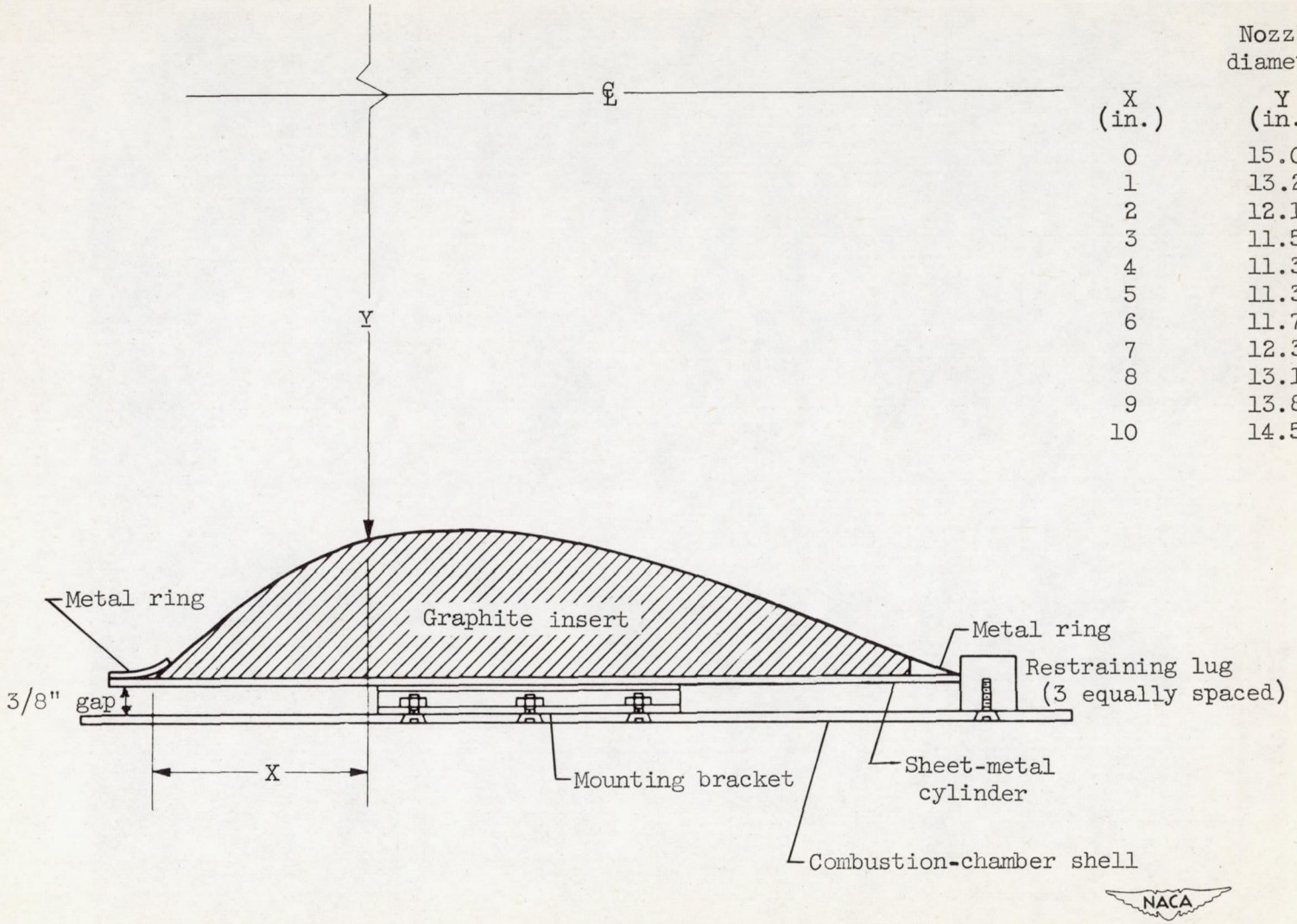

X (in.)	Nozzle diameter Y (in.)
0	15.08
1	13.28
2	12.18
3	11.50
4	11.31
5	11.32
6	11.70
7	12.38
8	13.12
9	13.80
10	14.55

Figure 7. - Primary-nozzle coordinates and mounting details.

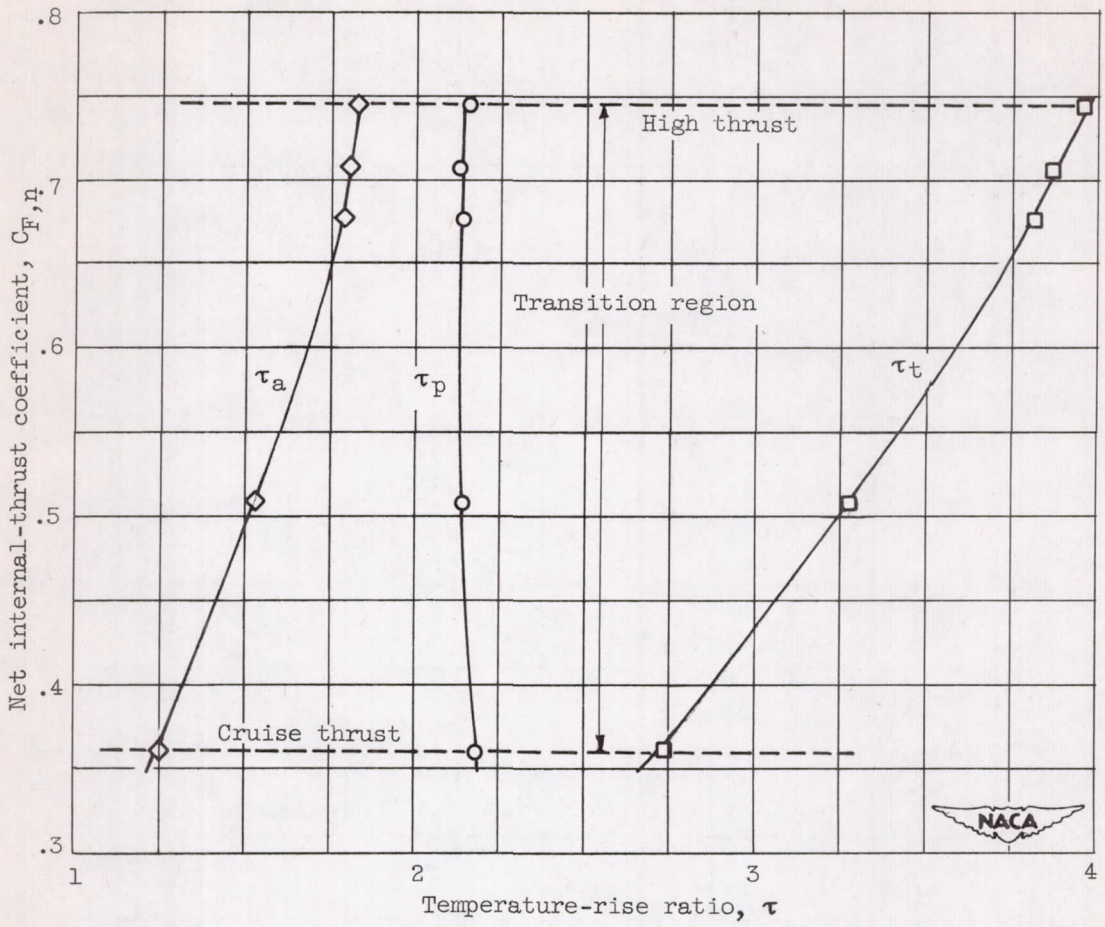

Figure 8. - Variation of net internal-thrust coefficient with total and component temperature-rise ratios. Free-stream Mach number M_0, 2.0; diffuser-exit Mach number M_3, 0.219±0.006; transition region primary fuel-air ratio, 0.038.

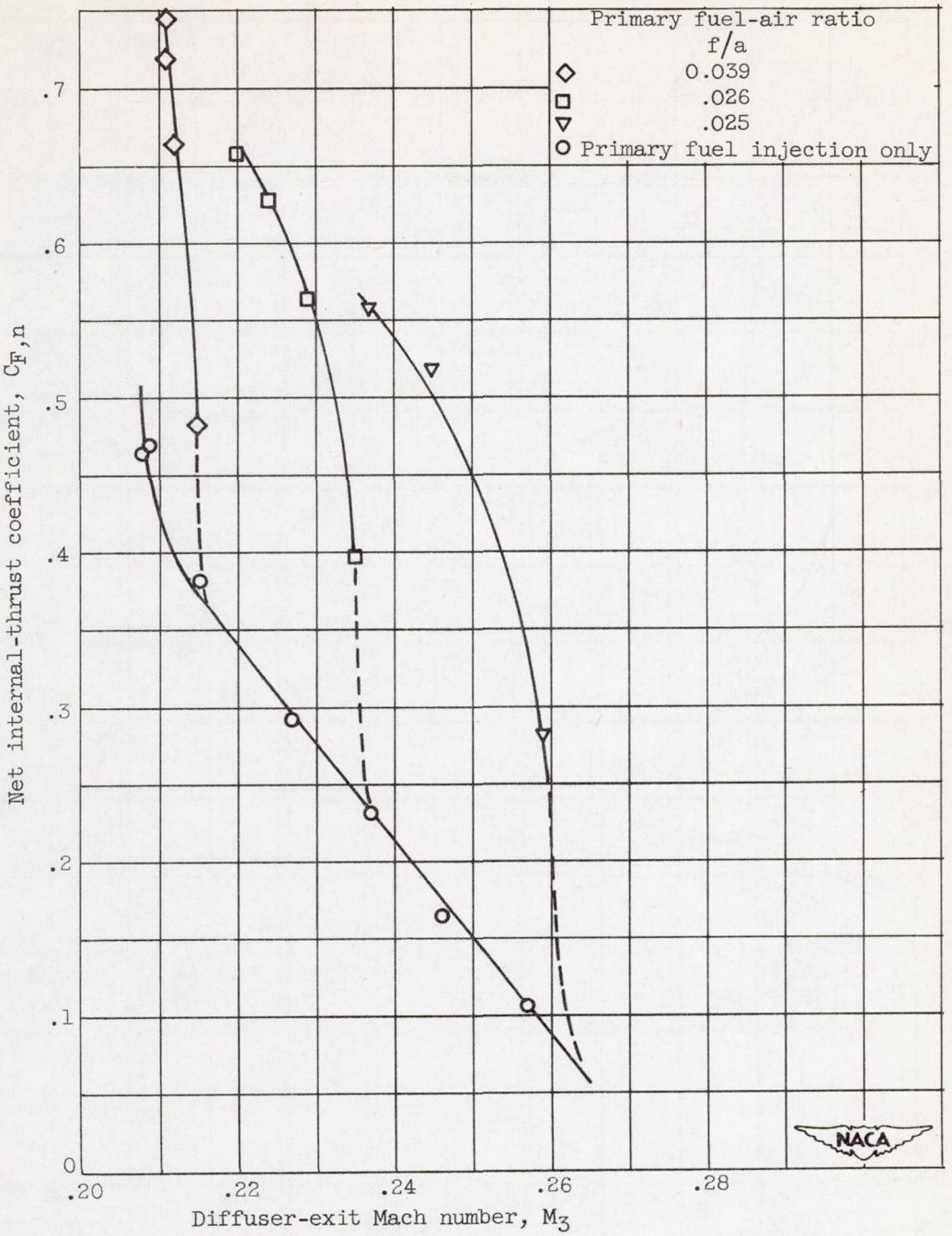

(a) Free-stream Mach number M_0, 1.8.

Figure 9. - Internal-thrust characteristics of afterburner-equipped ram-jet engine.

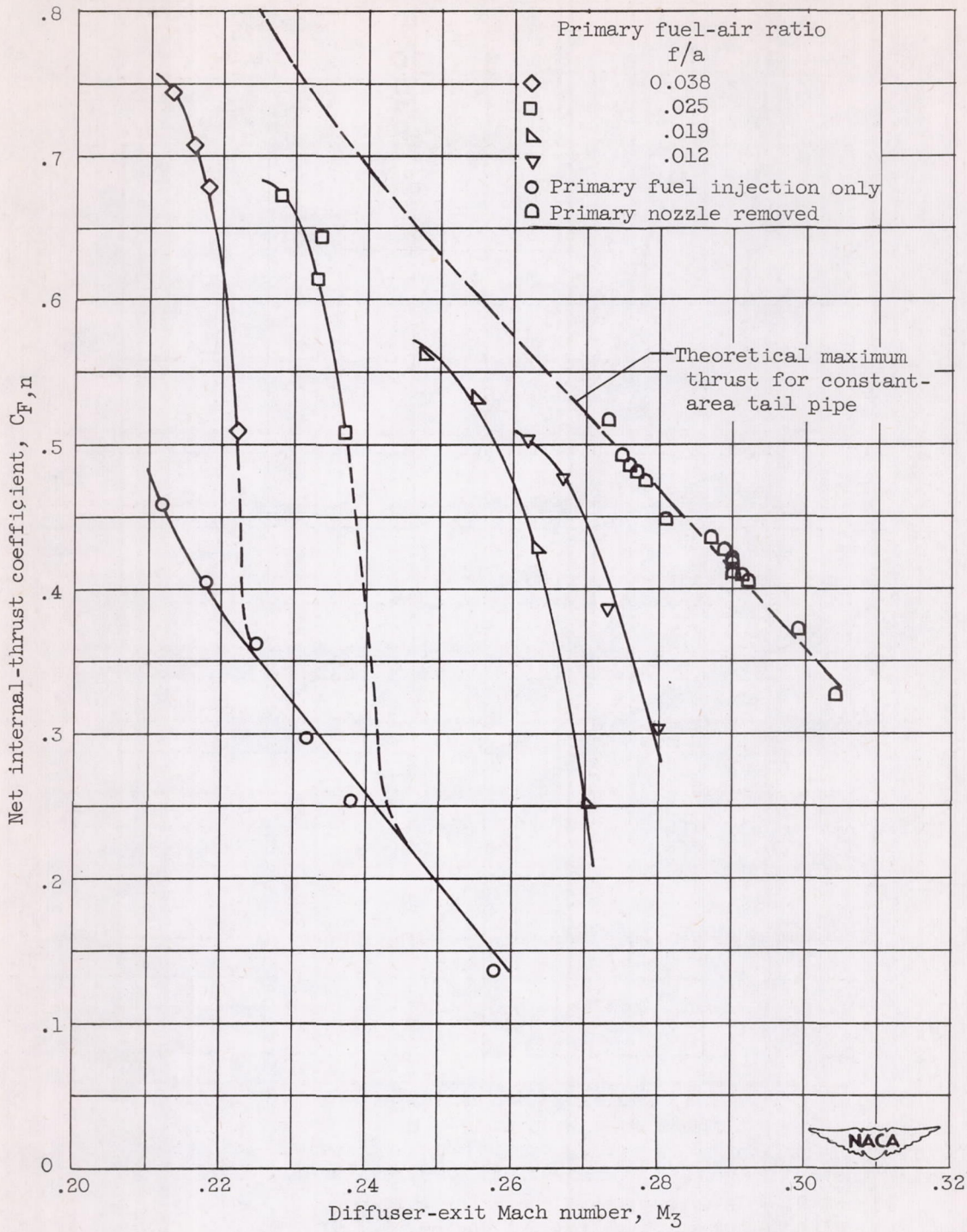

(b) Free-stream Mach number M_0, 2.0.

Figure 9. - Concluded. Internal-thrust characteristics of afterburner-equipped ram-jet engine.

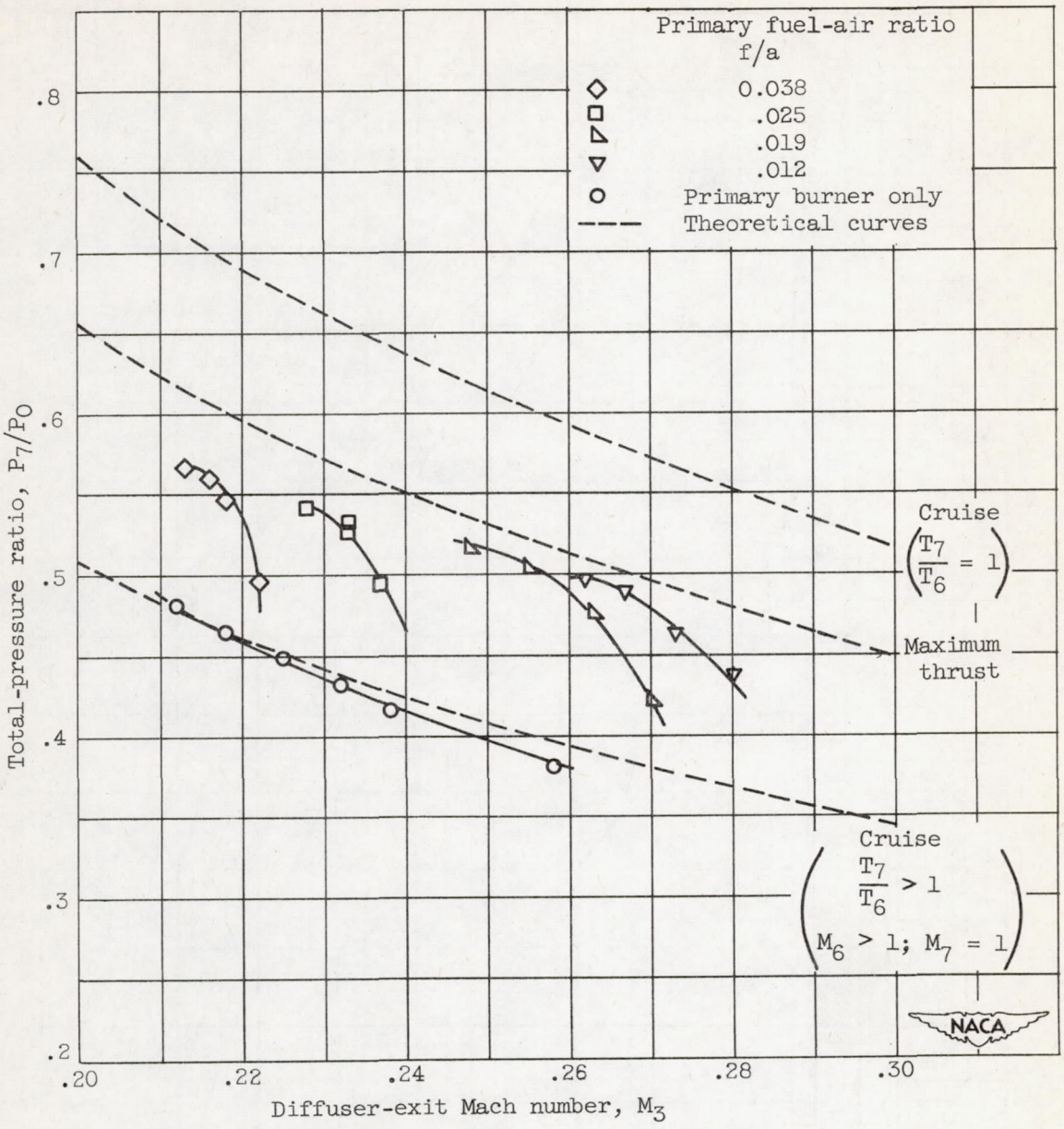

Figure 10. - Effect of operating conditions on the total-pressure ratio across the engine. Free-stream Mach number M_0, 2.0.

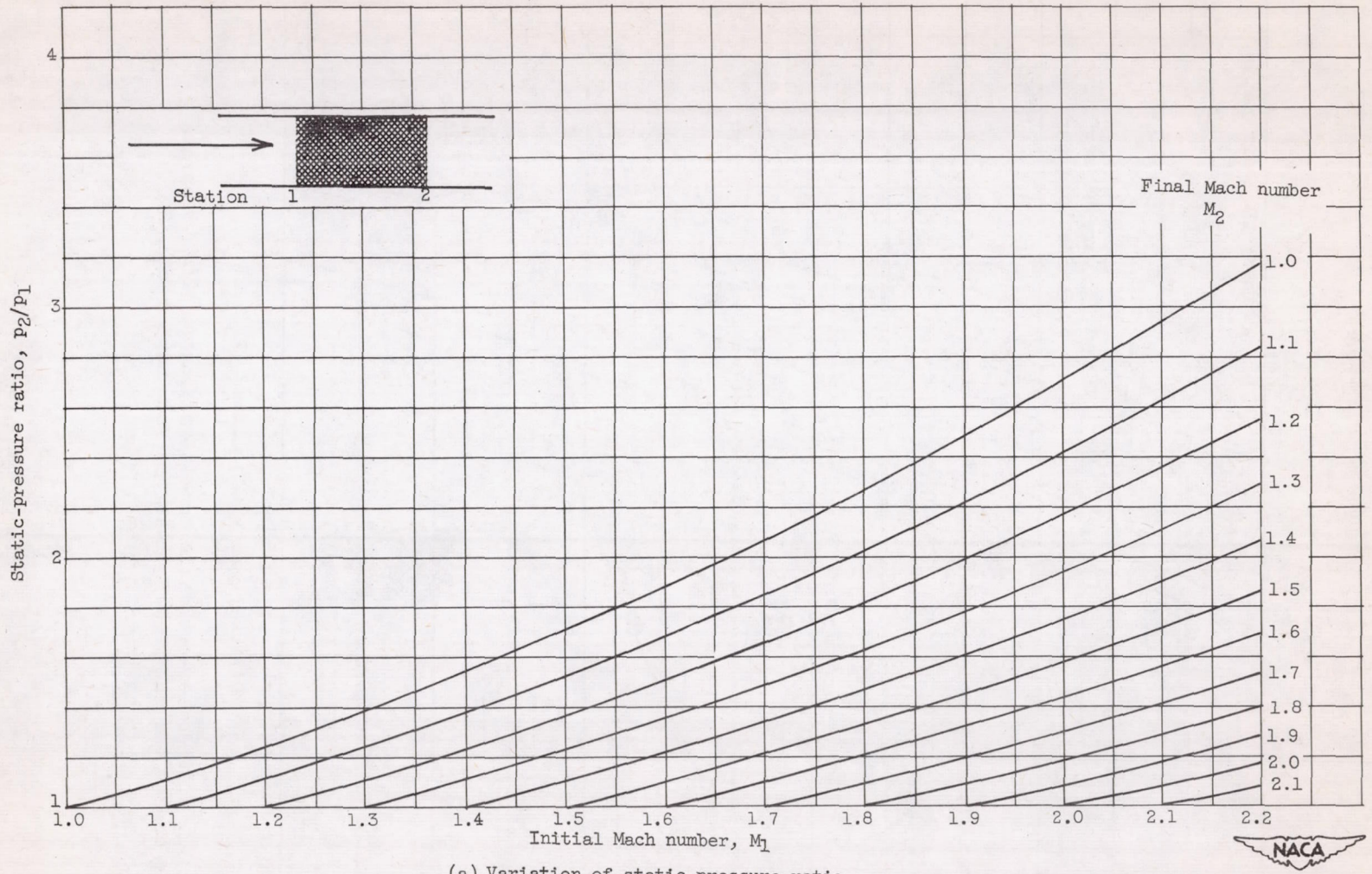

(a) Variation of static-pressure ratio.

Figure 11. - Supersonic heat-addition in constant-area duct. Initial Mach number $M_1 > 1$; ratios of specific heats γ_1 and γ_2, 1.3.

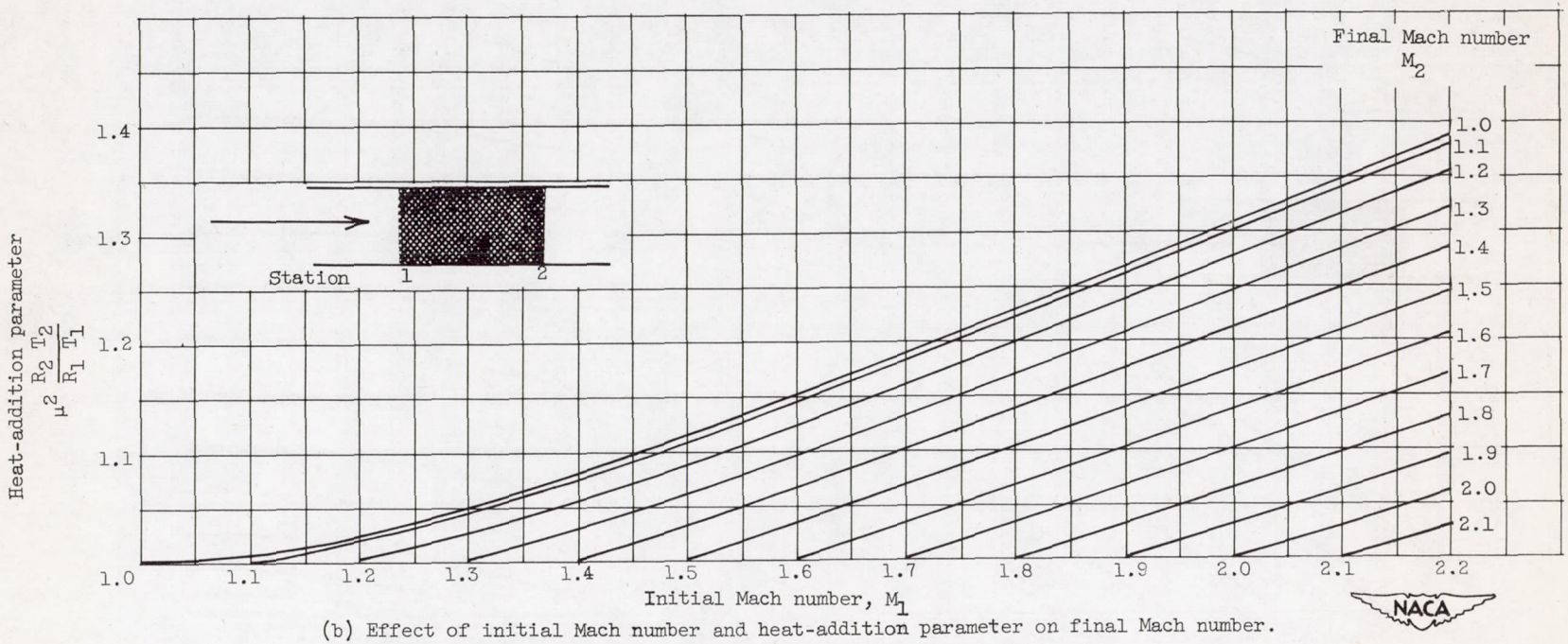

(b) Effect of initial Mach number and heat-addition parameter on final Mach number.

Figure 11. - Continued. Supersonic heat-addition in constant-area duct. Initial Mach number $M_1 > 1$; ratios of specific heats γ_1 and γ_2, 1.3.

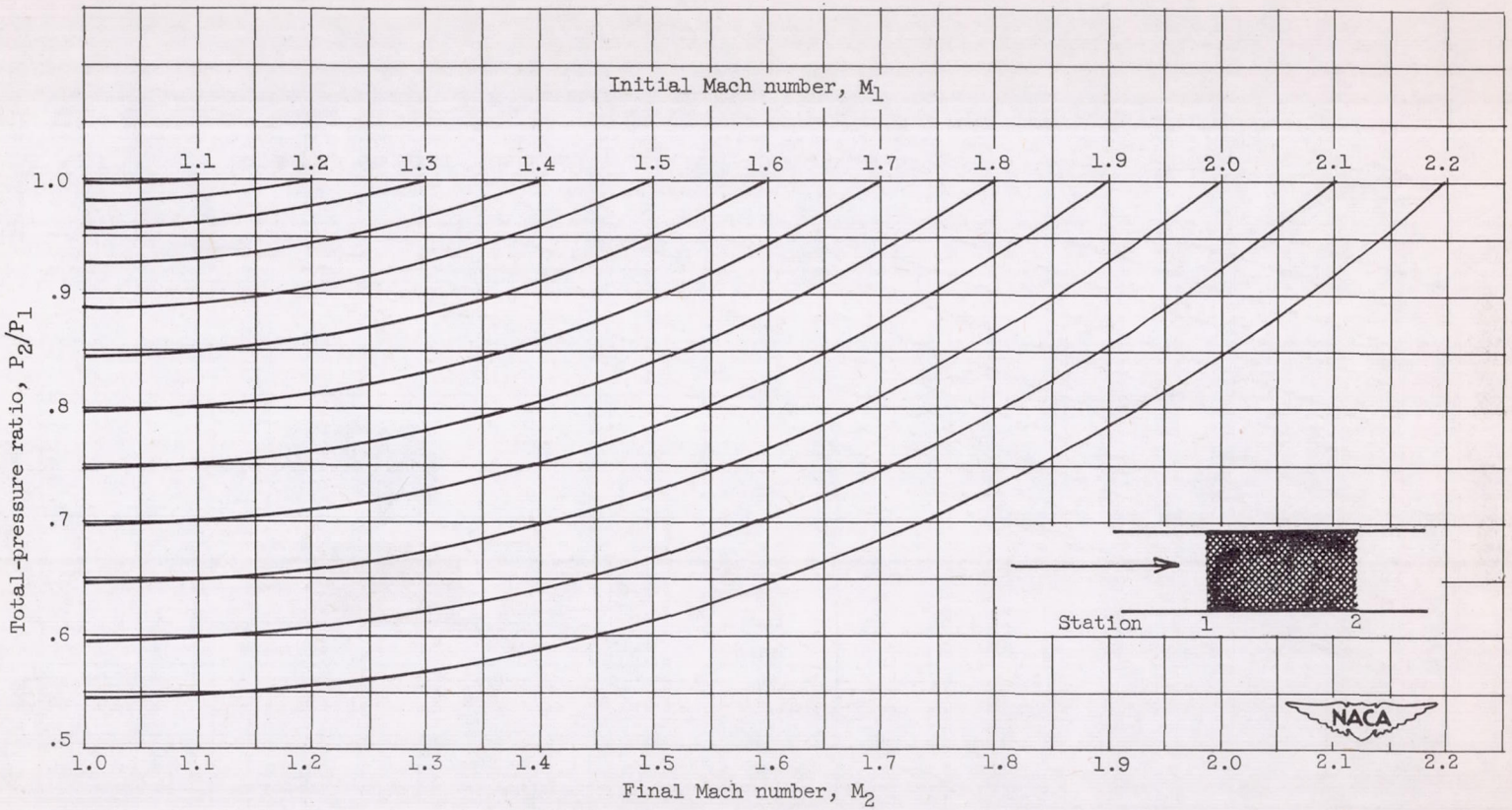

(c) Variation of total-pressure ratio.

Figure 11. - Continued. Supersonic heat-addition in constant-area duct. Initial Mach number $M_1 > 1$; ratios of specific heats γ_1 and γ_2, 1.3.

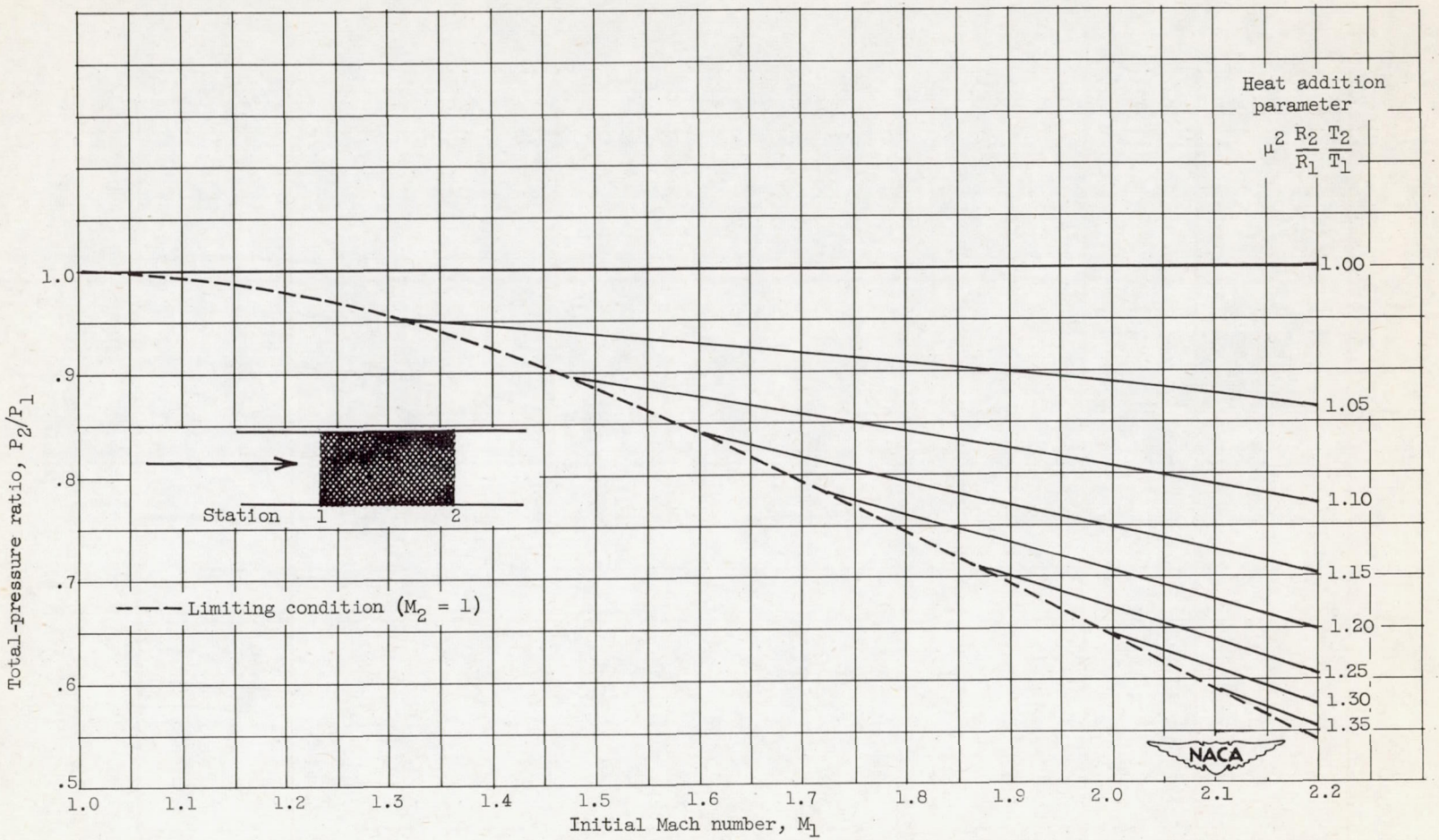

(d) Variation of total-pressure ratio across a constant-area duct with initial Mach number and heat-addition parameter.

Figure 11. - Concluded. Supersonic heat-addition in constant-area duct. Initial Mach number $M_1 > 1$; ratios of specific heats γ_1 and γ_2, 1.3.

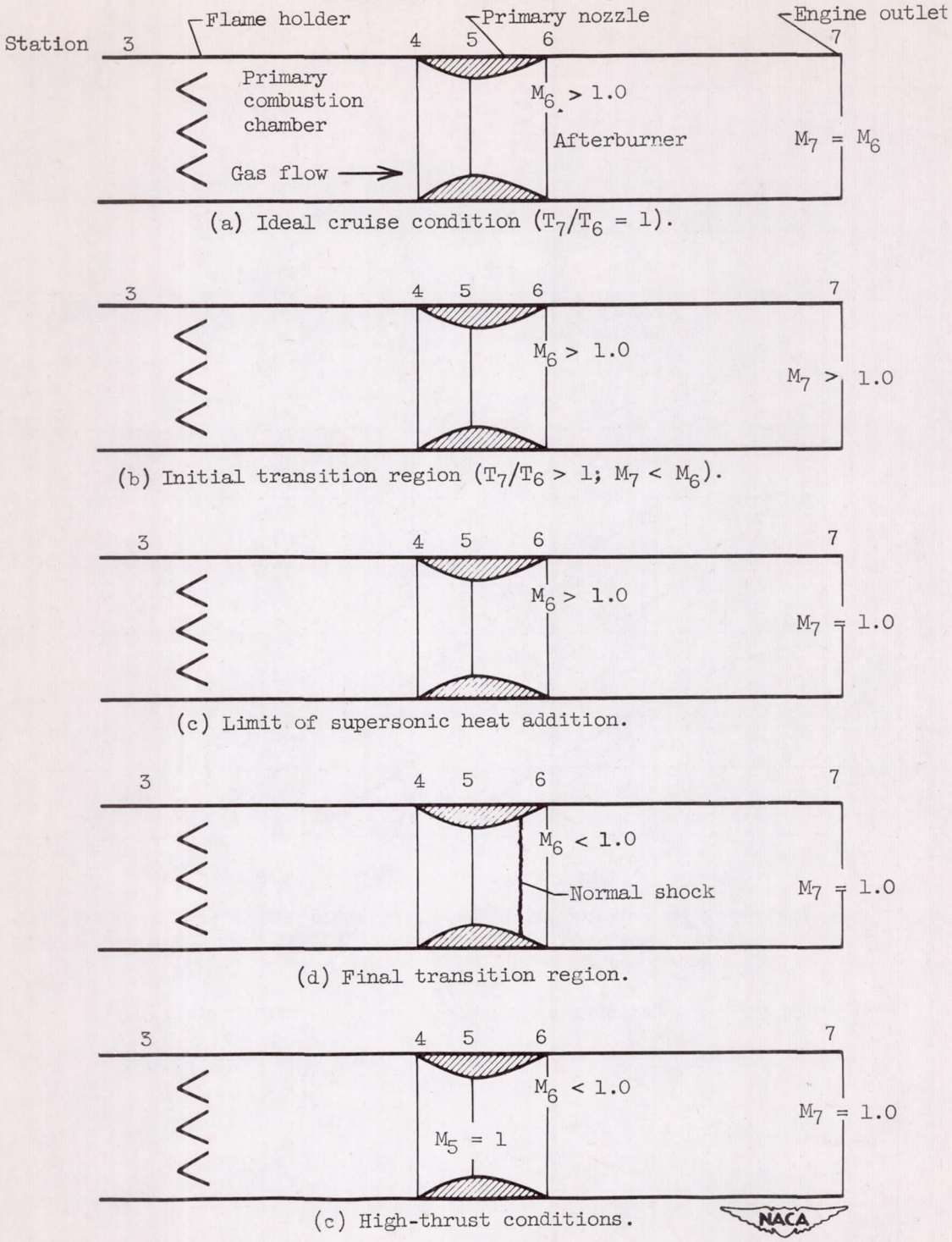

Figure 12. - Operating regions of ram-jet engine with afterburner. $M_4 < 1.0$; $M_5 = 1.0$.

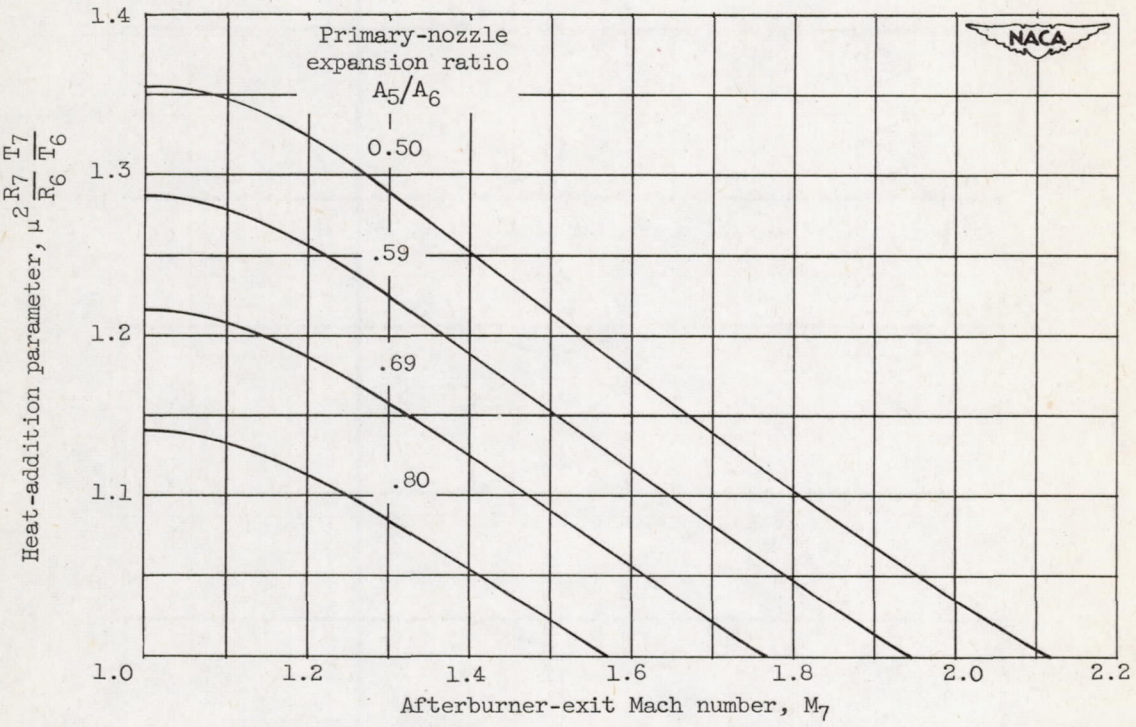

(a) Effect of primary-nozzle-expansion ratio and afterburner-exit Mach number on heat-addition parameter. Initial transition region. $T_5 = T_6$; $\gamma = 1.3$.

Figure 13. - Constant-area afterburner flow characteristics.

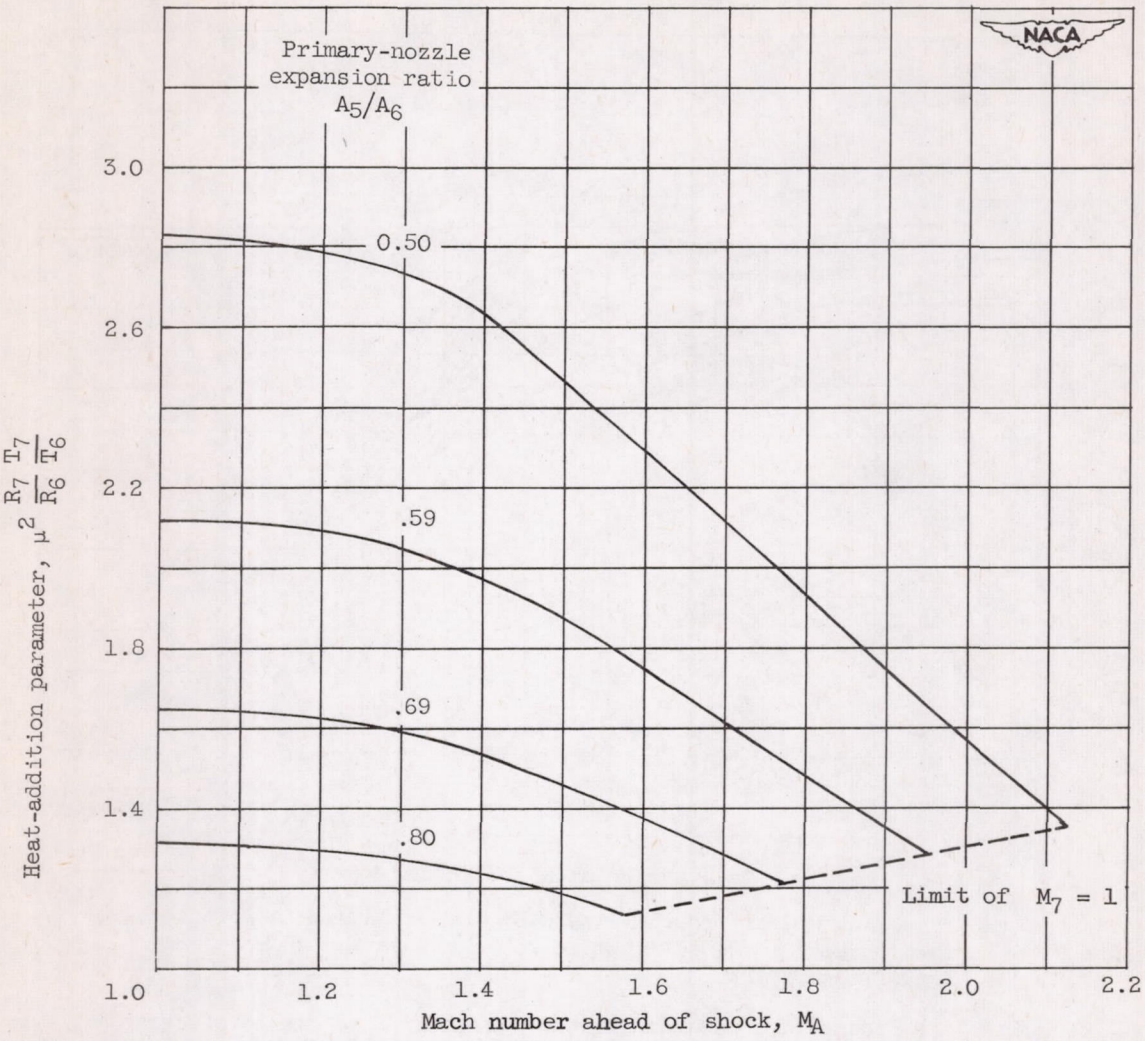

(b) Effect of primary-nozzle-expansion ratio and Mach number ahead of normal shock on heat-addition parameter. Final transition region. $M_5 = 1$; $M_7 = 1$; $T_5 = T_6$; $\gamma = 1.3$.

Figure 13. - Continued. Constant-area afterburner flow characteristics.

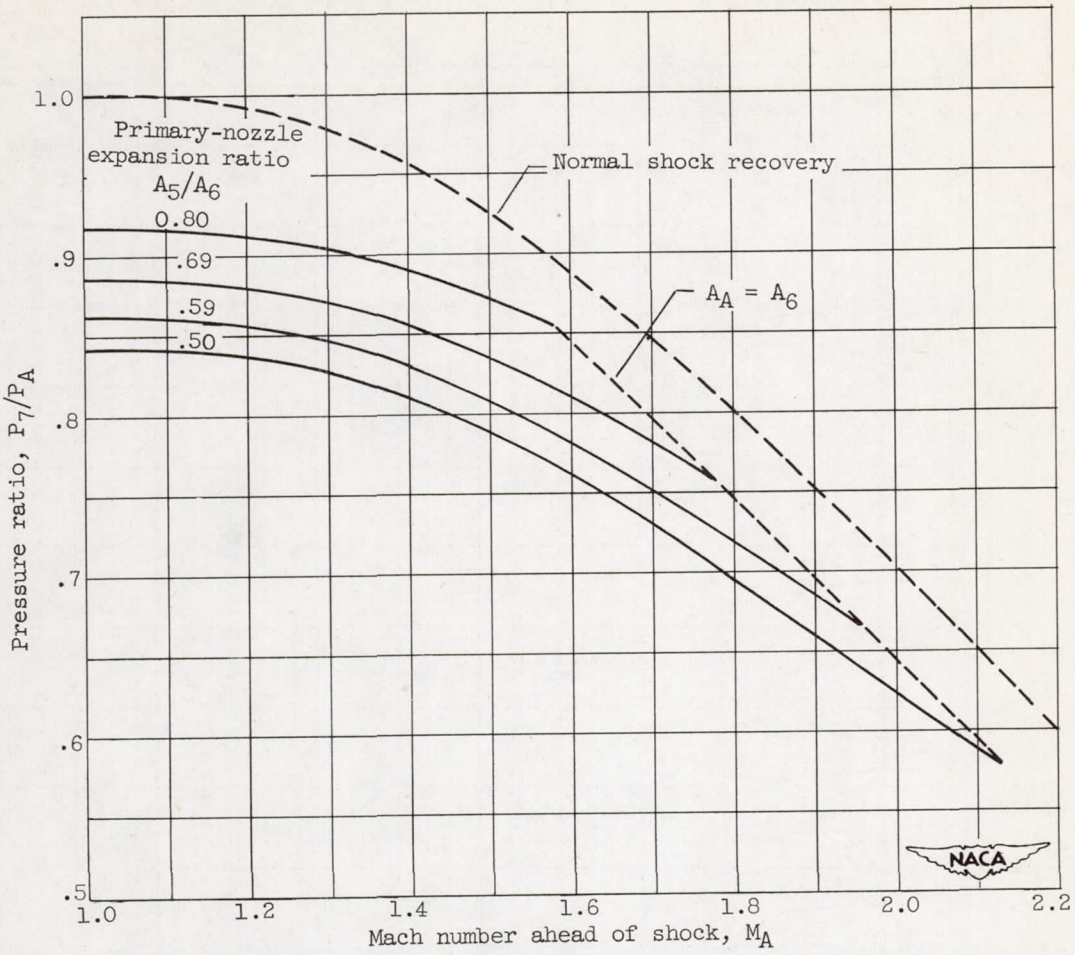

(c) Effect of primary-nozzle-expansion ratio and Mach number ahead of normal shock on total-pressure ratio across the afterburner. Transition region. $M_5 = 1$; $M_7 = 1$; $T_5 = T_6$; $\gamma = 1.3$.

Figure 13. - Concluded. Constant-area afterburner flow characteristics.